Ethylene–4-methyl-1-pentene copolymers of complex chain architecture using α-diimine Ni(II) catalysts: synthesis, ^{13}C NMR assignment and understanding the chain-walking mechanism†

Simona Losio,* Giuseppe Leone, Fabio Bertini, Giovanni Ricci, Maria Carmela Sacchi and Antonella Caterina Boccia*

Ethylene (E) and 4-methyl-1-pentene (4M1P) are copolymerized using an α-diimine Ni(II) catalyst with MAO (methylaluminoxane) or Et$_2$AlCl (diethylaluminium chloride) as the cocatalyst. A series of copolymers with a 4M1P comonomer content ranging from 0.94 to 36.73 mol% are obtained. A detailed ^{13}C NMR assignment is presented and this thorough analysis has opened up the first full description of this interesting family of copolymers. Manifold branched copolymers are obtained with no noticeable differences in the branching distribution by using MAO or Et$_2$AlCl. The resonance assignments are correlated with the chain-walking mechanism: branching analysis shows that the total amount of 2,1 insertion of the comonomer, followed by backward migration of the nickel active species along the polymer chain, is higher than that of 1,2 inserted 4M1P.
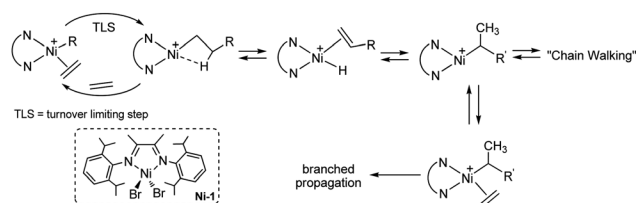
Introduction

One of the ultimate challenges in polymer science is the ability to fabricate polymers and block copolymers with well-defined stereochemistry, predictable molecular weight, and novel architecture, including dendrimers, branched and hyperbranched polymers.[1–4] Therefore, the development and understanding of synthetic strategies for the polymerization of a wide range of monomers is a central theme to synthesize materials with unique chain topologies and striking properties. With regard to polyolefins, most of the synthetic approaches involve the addition polymerization (*i.e.*, ionic, radical, coordination–insertion and so on) of vinyl monomers in which the active growing site stays at the end of macromolecule chains, and the successive monomer additions lead to the formation of linear structures. A fascinating strategy to fabricate branched and hyperbranched polyolefins with unique chain architecture comes from the use of chain walking catalysts by a coordination–insertion polymerization mechanism.[5–8] The peculiarity of these catalytic systems is attributed to the ability of the active growing site to "walk" on the polymer chain during the propagation step, so that the new incoming monomer unit is assembled onto the polymer backbone rather than at the end.

This nonlinear manner of the chain propagation allowed the synthesis of polyolefins with various branching topologies. Scheme 1 briefly summarizes the general chain walking mechanism for ethylene polymerization.[9]

Compared with traditional linear polyolefins, the synthesis of a polymer with a branched chain topology offers the potential to increase polyolefin melt fracture resistance, paintability, elasticity, and compatibility with other materials. This extraordinary opportunity in the field of polyolefins chemistry is possible thanks to the discovery of new and highly robust α-diimine Ni(II) and Pd(II) metal complexes by Brookhart and coworkers. These complexes, in combination with aluminium alkyls or borate activators, are unique in their ability to fabricate polyolefins with non-linear architecture.[9–12] The subsequent and rapid development of chemistry of the late metal based catalysts has stimulated the evolvement of polymers and block copolymers from ethylene (E), linear α-olefins, *i.e.*, propylene (P) and

ISMAC, Via Bassini, 15, 20133 Milano, Italy. E-mail: s.losio@ismac.cnr.it; antonella. boccia@ismac.cnr.it; Fax: +39 0270636400; +39 0223699620; Tel: +39 0223699366; +39 0223699212

† Electronic supplementary information (ESI) available: ^{1}H, ^{1}H–^{1}H TOCSY, and ^{1}H–^{1}H COSY experiments of run 6 in Table 1. A T_g plot for runs 1–6. Ethyl, propyl, and butyl branch distribution. See DOI: 10.1039/c3py01508d

Scheme 1 General mechanism for the ethylene polymerization and polymer branch formation by chain walking with Ni(II) α-diimine complexes. The structure of a **Ni-1** complex is shown in the rounded rectangle box.

1-hexene (1-Hex), and branched α-olefins, *i.e.*, 4-methyl-1-pentene (4M1P).[13–25] In this scenario, we recently first reported a brief communication (*Polym. Chem*, **3**, 2012, 1987) on the copolymerization of E with 4M1P catalyzed by [ArN=C(CH₃)–(CH₃)C=NAr]NiBr₂ with Ar = 2,6-(ⁱPr)₂C₆H₃ (compound **Ni-1**) and diethylaluminium chloride (Et₂AlCl).[26] At low temperature, living copolymerization was attained, with a linear increase of the poly(E-*co*-4M1P) molecular weight while maintaining a low dispersity ($M_w/M_n \approx 1.1$). This feature enabled the synthesis of a range of poly(E-*co*-4M1P)-*block*-poly(1-Hex).

In this work, we continued our investigation on the Ni α-diimine-catalyzed polymerization of E with 4M1P; specifically (i) we examined the use of the **Ni-1** complex in combination with MAO and the fabrication of copolymers with a broader range of 4M1P incorporation (from 1 to 36 mol%) and (ii) we carried out a detailed microstructural investigation (*i.e.*, composition, sequence distribution, branch type, frequency, and type of insertion) by applying the gradient-assisted 2D NMR techniques, *i.e.*, g-HSQC (heteronuclear single quantum correlation) and g-HMBC (heteronuclear multiple bond correlation).[27–29] In light of previous and new findings, we present a set of resonance assignments that we have correlated with the chain-walking mechanism involved in the copolymerization of E with 4M1P by α-diimine Ni based catalysts.

Experimental section

General considerations and materials

Manipulations of air- and/or moisture-sensitive materials were carried out under an inert atmosphere using dual vacuum/nitrogen line and standard Schlenk-line techniques. Toluene (Fluka, >99.5% pure) was refluxed over Na for *ca.* 8 h and then distilled and stored over molecular sieves under nitrogen. Methylalumoxane (MAO) was used after removing all volatiles and drying the resulting powder at 50 °C for 3 h in a vacuum. Diethylaluminium chloride (Et₂AlCl) (Fluka) was used as received. Nickel(ɪɪ) complex [ArN=C(CH₃)–(CH₃)C=NAr]NiBr₂ (Ar = 2,6-(ⁱPr)₂C₆H₃) (**Ni-1**) was synthesized according to the experimental procedures previously reported in the literature.[11] 4-Methyl-1-pentene (4M1P) (Aldrich) was refluxed over CaH₂ for about 2 hours, then distilled trap-to-trap and, finally, stored under dry nitrogen and kept at −20 °C. Ethylene was purified by allowing to flow through BTS catalysts, molecular sieves, and CaCl₂. A deuterated solvent for NMR measurements (C₂D₂Cl₄) (Cambridge Isotope Laboratories, Inc.) was used as received.

Polymerization procedure

The polymerization experiments were carried out in a 25 mL round-bottomed Schlenk flask containing a stirring bar. The polymerization reactor was first dried by heating at 80 °C and then a vacuum was applied for 1 h at 40 °C.

Ethylene/4-methyl-1-pentene copolymerization. The reactor vessel was charged with 4M1P and toluene and the solution was brought to the desired polymerization temperature. Et₂AlCl or MAO was added and the solution was degassed and saturated with ethylene under vigorous stirring for 10 min. The

polymerization was started by adding a toluene solution of the nickel compound under continuous flow of ethylene. Polymerization was stopped with methanol containing a small amount of hydrochloric acid; the precipitated polymers were collected by filtration, repeatedly washed with fresh methanol, and then dried in a vacuum at room temperature to constant weight.

Polymer characterization

Nuclear magnetic resonance spectroscopy (NMR). ¹³C NMR experiments were performed on a Bruker Avance 400 spectrometer at 100 MHz, using a 10 mm broadband probe, at 100 °C, and on a Bruker DMX 600 spectrometer equipped with a 5 mm PFG probe working at 60 °C. Samples were dissolved in TCE (1,1,2,2-tetrachloroethane-d₂), and referenced to the internal HMDS (hexamethyldisiloxane) signal. The concentration of the polymer solution was about 10 wt%. For a quantitative analysis the experimental parameters were set as follows: ¹H conditions – 90° pulse: 8.35 μs; ¹³C – 90° pulse: 11 μs, relaxation delay: 16 s, acquisition time: 4.32 s, 7.5 kHz spectral width.

¹³C DEPT NMR spectra were measured applying a standard dept_135 library sequence, with a delay of 6 s, and a 90° pulse width of 14.5 μs, −4.0 dB, for ¹³C and 98.00 μs, 7.0 dB, for ¹H.

g-HSQC experiments were carried out with a delay of 1.79 ms, corresponding to a ¹J_CH = 140 Hz. g-HMBC experiments, with 2-fold low-pass J-filter, were carried out with a delay of 100 ms for the evolution of long-range coupling, and delays corresponding to ¹J_CH = 130 and 160 Hz.

Molecular analysis

The molecular weight averages (M_n) and the molecular weight distribution (M_w/M_n) were obtained by a high temperature Waters GPCV2000 size exclusion chromatography (SEC) system using two online detectors: a differential viscometer and a refractometer. The experimental conditions consisted of three PL Gel Olexis columns, *o*-DCB as the mobile phase, 0.8 mL min⁻¹ flow rate, and 145 °C temperature. Universal calibration of the SEC system was performed using eighteen narrow M_w/M_n polystyrene standards with molar weights ranging from 162 to 5.6×10^6 g mol⁻¹. For the analysis, about 12 mg of the polymer was dissolved in 5 mL of *o*-DCB with 0.05% of BHT as the antioxidant.

Thermal analysis

Differential scanning calorimetry (DSC) scans were carried out on a Perkin-Elmer Pyris 1 instrument equipped with a liquid nitrogen device. Typically, *ca.* 5 mg of the polymer were analyzed in each run, at a scan rate of 20 °C min⁻¹ under a helium atmosphere. T_g was recorded during a second thermal cycle.

Results and discussion

As reported in our earlier communication, copolymerization of E with 4M1P with catalyst **Ni-1**, in combination with Et₂AlCl, results in a poly(E-*co*-4M1P) with high catalytic activity.[26] The copolymerization proceeds in a living manner at 0 °C, affording a narrow polymer molecular weight distribution ($M_w/M_n \approx 1.1$)

although the observed 4M1P comonomer incorporation was somewhat lower than those reported, for instance, with metallocene and half-titanocene based catalysts.[30–34]

The **Ni-1**–Et$_2$AlCl system was also used to prepare block copolymers by sequential 1-hexene monomer addition. Amorphous, highly branched poly(E-*co*-4M1P)-*block*-poly(1-Hex)s with a M_w/M_n of 1.2 were readily produced.[26]

The results obtained led us to investigate the copolymerization in detail under a broad range of experimental conditions. Thus, reactions were carried out at 0 and 20 °C in a wide E/4M1P mole ratio range. In Table 1, three series of experiments are reported and compared. The first series was conducted by using MAO cocatalyst at room temperature and constant polymerization time, in a wide E/4M1P mole ratio range (1.1–21.8). The second series of experiments was conducted with MAO cocatalyst, at 0 °C and constant E/4M1P mole ratio range (1.1), while the polymerization time was increased from 1 to 8 min. The third series consisted in three experiments (two of them, runs 13 and 14, are reported in ref. 26) conducted with an Et$_2$AlCl cocatalyst under different polymerization conditions that are useful in comparing the effects of MAO and Et$_2$AlCl cocatalysts on the copolymerization behaviour. Two samples of polyethylene prepared under the conditions of the first and the third series (runs 1 and 11 in Table 1) are also presented as points of reference. 4M1P homopolymerization was performed with low yields. As a consequence, the authors take as reference data from the literature.[14,15]

In the series of experiments carried out at room temperature and different feedstock compositions (runs 2–6), we can observe that, on increasing the amount of 4M1P in the feed, the 4M1P incorporation in the copolymer increases linearly up to about 30 mol% of the comonomer ([4M1P] in the feed: 1.66 mol L^{-1}). With a [4M1P] higher than 2.45, the comonomer incorporation levelled off as shown in Fig. 1a. Moreover, under the conditions employed, the glass transition temperatures (T_gs) increase with

4M1P content, changing from −65 to −57 °C for a 4M1P content from 0 to 36.73 mol%, respectively (Fig. 1b). When polymerizations were carried out at 0 °C (runs 7–10), poly(E-*co*-4M1P)s with noticeable lower M_w and less efficient 4M1P incorporation were obtained. The decreasing 4M1P insertion rate with respect to the E, as expected, is consistent with the increased ethylene solubility at low temperature.[35] As to the polymerization living character, in general, where MAO compound was employed instead of Et$_2$AlCl, the M_w/M_n increased, suggesting a certain extent of chain transfer reaction. Specifically, with **Ni-1**–MAO a M_w/M_n of 1.73 ($M_w = 10.9 \times 10^4$) was achieved just before 8 min of reaction (run 10), whereas with **Ni-1**–Et$_2$AlCl the preservation of narrow M_w/M_n (≈ 1.2) with increase in the reaction time over 25 min (run 12) indicated a long life-time living/controlled polymerization. This result, in accordance with the literature, arises from the occurrence of growing chain transfer to trimethylaluminum (TMA), which is contained in the commercially available MAO. However, the temperature also seems to exert a moderate effect on the living polymerization behaviour: indeed, in the series of experiments conducted at 0 °C, M_w/M_n is always less than 2, even if with some fluctuations, and a gradual increase of the molecular weights with polymerization time can be detected.[36]

^{13}C NMR assignments

Assignments shown on the NMR spectra are labelled according to Schemes 2 and 3. The nomenclature used in this work for isolated branches is that of Usami and Takayama:[37]

- xBy: By is a branch of length y carbons and x is the carbon number starting with the methyl groups as "1". For the backbone carbons, Greek letters and "br" are used instead of x for the methylenes and a branch point, respectively. For example, 1B$_1$ designates the methyl in a methyl branch, 2B$_2$ the methylene carbon in an ethyl branch, and γB$_2$ the backbone carbon in the γ-position from an ethyl branch. For paired branches

Table 1 Copolymerization of E with 4M1P by **Ni-1**–MAO and **Ni-1**–Et$_2$AlCl[a]

Run	4M1P[b] (mol L^{-1})	[4M1P]/[E][c]	Al-alkyl (type)	T (°C)	Time (min)	Yield (g)	Activity[d]	4M1P[e] (mol%)	$M_w{}^f \times 10^4$	$M_w/M_n{}^f$	$T_g{}^g$ (°C)
1	—	—	MAO	20	25	1.74	418	—	21.04	1.83	−65
2	0.16	1.1	MAO	20	25	1.56	374	4.87	22.70	2.00	−63
3	0.55	3.8	MAO	20	25	1.20	288	10.40	18.40	2.50	−62
4	1.66	11.5	MAO	20	25	1.30	312	30.06	15.80	1.40	−61
5	2.45	16.9	MAO	20	25	0.82	197	33.52	19.90	1.53	−59
6	3.17	21.8	MAO	20	25	0.79	190	36.73	16.80	1.56	−57
7	0.26	1.1	MAO	0	1	0.03	180	0.94	3.01	1.34	
8	0.26	1.1	MAO	0	2	0.10	300	2.32	4.46	1.46	
9	0.26	1.1	MAO	0	4	0.24	360	2.13	7.46	1.73	
10	0.26	1.1	MAO	0	8	0.56	420	3.29	10.9	1.73	
11	—	—	Et$_2$AlCl	20	25	1.00	238	—	10.2	2.17	
12	2.45	16.9	Et$_2$AlCl	20	25	0.90	216	31.65	13.2	1.38	−60
13[h]	0.55	3.4	Et$_2$AlCl	20	15	0.53	212	15.41	4.76	1.29	
14[h]	0.55	2.3	Et$_2$AlCl	0	15	0.79	317	5.60	6.82	1.13	

[a] Polymerization conditions: **Ni-1**, 10 μmol; PE = 1.01 bar; runs 1–6, Al/Ni = 500; runs 7–12, Al/Ni = 200; runs 1–6, 11 and 12, [Ni] = 2 × 10^{-4} mol L^{-1}; toluene, 50 mL total volume; runs 7–10, [Ni] = 6.25 × 10^{-4} mol L^{-1}; toluene, 16 mL total volume. [b] 4M1P feed concentration. [c] [4M1P]/[E], feed monomer molar ratio. [d] kg$_{polymer}$/(mol$_{Ni}{}^{-1}$ × h^{-1}). [e] From ^{13}C NMR. [f] From SEC in *o*-DCB by using universal calibration. [g] From DSC, second heating. [h] From ref. 26.
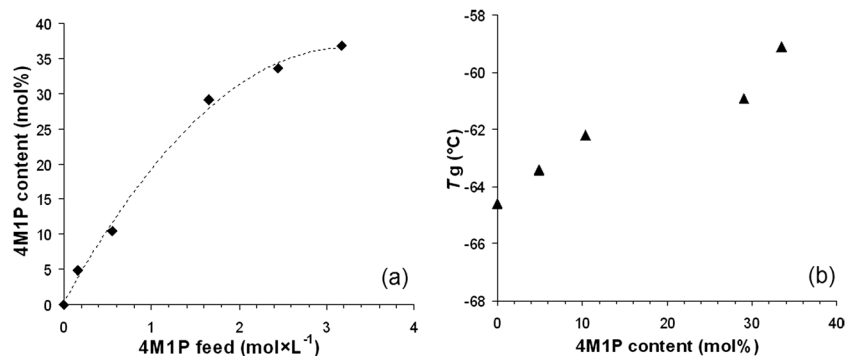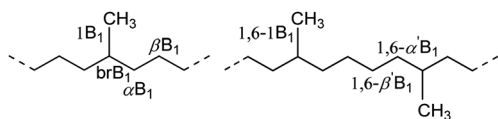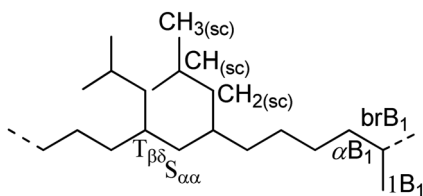
Fig. 1 Plot of 4M1P content *vs* 4M1P feed (a) and T_g *vs* 4M1P content (b) for runs 1–6.

Scheme 2 Branching nomenclature.

Scheme 3 Structure and carbon numbering of an E–4M1P copolymer from catalyst **Ni-1**.

prefixes 1,*m* are used, where *m* is the number of carbons between two tertiary carbons, 1 being the first tertiary carbon and *m* the next. The backbone carbons between branches are designated by Greek letters with primes.

- Methyl, methylene and methine carbons in a 4M1P side chain are designated by the symbols $CH_3(sc)$, $CH_2(sc)$, and $CH(sc)$.

- For the backbone, the carbon terminology follows that of Carman and Wilkes, where P, S, and T refer respectively to the primary (methyl), secondary (methylene), and tertiary (methine) carbons of the main chain.[38] The two Greek subscripts indicate the distances of the carbon in question from the neighbouring methines, where δ indicates all methines farther than three bonds from the methylene carbon of interest (Scheme 3).

In the following, "E" and "Y" indicate the ethylene and 4M1P comonomer units, respectively, in the description of monomer sequence distribution. The branching structure of the E–4M1P copolymers produced by **Ni-1** based catalysts is singled out and analyzed to study the relationship between polymer micro-structure and chain-walking mechanism. The ^{13}C NMR spectra of copolymers with different comonomer contents, *i.e.*, 10.40 and 36.73 mol%, respectively, and PE, are shown in Fig. 2. In agreement with previous work from Galland *et al.*, highly branched E sequences resulting from catalyst chain walking, in

the presence of branch length ranging from methyl to hexyl and longer, are easily detected in Fig. 2a.[39,40] By analyzing Fig. 2b and c, a branched structure of the copolymers can be safely identified, as for the PE.

To shed light on the peculiar structure of the copolymers, we performed a ^{13}C NMR characterization by combining previous E–4M1P copolymer assignments and referencing to model compound data found in the literature.[30–32,41] The set of NMR resonances was compared with DEPT-135 data, Fig. 3, to discriminate carbon signals. Indeed, methylene carbons appear 180° opposite in phase (negative) with respect to methyl and methine carbons (positive).

According to the literature and by comparing the spectrum of Fig. 2b with that of PE, the signal at 12.01 ppm should be assigned to methyl carbons of longer branches ($1B_4$, $1B_5$, and $1B_n$). However, after a careful analysis, we assigned that signal only to $1B_4$ branches. The main reason for this assignment derives from the absence in the ^{13}C spectra of the expected resonances $2B_5$ and $2B_n$ at 20.69 ppm (methylenes adjacent to the methyl at 12.01 ppm),[39] because the DEPT experiment puts in evidence that the resonance at 20.69 ppm is a primary carbon. Such a comparison also evidences that short methyl branches, ascribed to the signal at 17.87 ppm, namely B_1 (*i.e.*, $1B_1$, $1,4\text{-}B_1$, $1,5\text{-}B_1$, and $1,6\text{-}B_1$), are the most common ones. These short branches were already observed in ^{13}C NMR spectra of poly(4M1P) from similar Ni(II) catalysts. Otherwise, 1,4-paired long branch units ($1,4\text{-}B_n$) or 1,4-paired long branches-on-branches unit, observed in the spectra of poly(4M1P) by α-dii-mine palladium catalysts, were not detected.[16,41]

Starting from previous E–4M1P assignments, at low como-nomer content, it is easy to identify, in Fig. 2b, the resonances corresponding to 4M1P units $CH_3(sc)$, $CH(sc)$ and $CH_2(sc)$ at 21.18, 23.75, and 42.50 ppm, respectively (Scheme 3).[30–32] At low 4M1P content, isolated comonomer units are mainly present because only βδ methylene and δδ methine carbons at 24.84 and 33.62 ppm, belonging to the EYEEE, are detected; αδ and γδ methylenes of the same sequence are not distinctively seen in the spectrum, at 32.54 and 28.23 ppm, due to the overlap with signals resulting from the highly branched ethylene sequences.

By increasing the 4M1P content up to *ca.* 36 mol%, in Fig. 2c, longer 4M1P sequences are detected too.[30–32] Indeed, the pres-ence of the YYE triad is confirmed by the resonance at 31.29
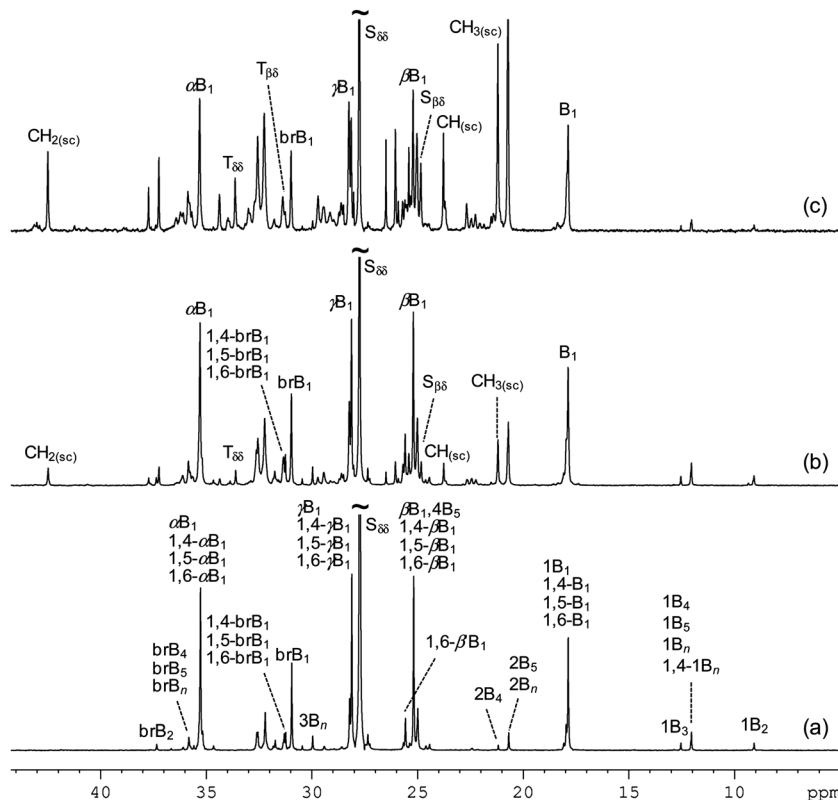
Fig. 2 ^{13}C NMR assignments for E−4M1P copolymers with different comonomer contents: (b) 10.40 mol% (run 3 in Table 1), (c) 36.73 mol% (run 6 in Table 1). The spectrum of PE (a) is reported as a reference (run 1 in Table 1).
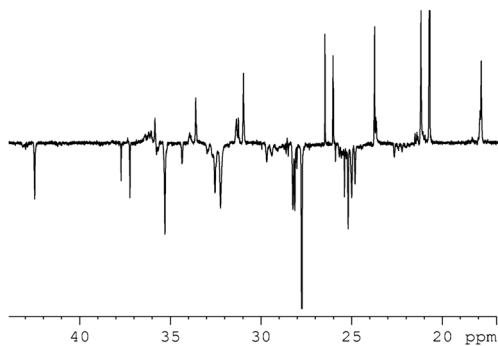

**Fig. 3** ^{13}C NMR DEPT spectrum of an E−4M1P copolymer with 36.73 mol% comonomer content (run 6 in Table 1).

ppm, assigned to $T_{\beta\delta}$, and by those of the signals ranging from 42.90 to 43.12 ppm assigned to $CH_2(sc)$ (see Scheme 3). Both these resonances are expected to have almost the same amplitude, as they belong to the same monomer enchainment sequence. Nevertheless, the integral of βδ methine carbon appears higher than that of the corresponding $CH_2(sc)$, due to the overlap with signals namely 1,5-brB$_1$ and 1,6-brB$_1$, ascribed to the highly branched E sequences.[39,40]

A careful analysis of the region corresponding to the three different YY centered tetrads (E*YY*E, Y*YY*E and Y*YY*Y as shown in Scheme 4) points out that none of the E/Y copolymers show αα methylene resonances ranging from 39.66 to 40.43 ppm;

therefore, the E*YY*E tetrad at 38.87 ppm is the only detectable tetrad. The lack of the Y*YY*γ tetrads (where γ means Y or E) is further confirmed by the absence of $T_{\beta\beta}$ carbons in the range from 29.04 to 29.42 ppm.

Even though methyl branches are the most common branches, none of the copolymers showed PY centered tetrads, where P is a propene unit, due to the absence of αα-methylene carbon atoms at 41.80 ppm (Scheme 5).[43]

The ^{13}C spectra in Fig. 2b and c showed a methyl carbon at 20.69 ppm, absent in the PE spectrum, whose intensity increased at higher comonomer content, thus suggesting that this resonance comes from 4M1P. For the assignment of this resonance, the authors consider that such a signal is not present in E/4M1P copolymer spectra from metallocenes and constrained geometry catalysts, and that methyl branches are the result of the chain-walking mechanism involved in the homopolymerization of 4M1P by α-diimine Ni(II) catalysts.[14,15,30–32] Thus, hereafter, we refer to the methyl carbon at 20.69 ppm as $CH_{3(CW)}$.
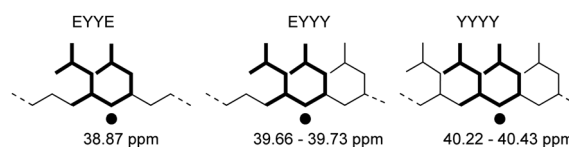
Scheme 4 Three possible YY centred tetrads and their distinctive chemical shifts.
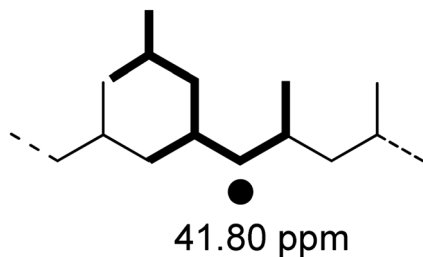
Scheme 5 $\alpha\alpha$ methylene carbon and its distinctive chemical shift.

To characterize the copolymer microstructure by 2D NMR analysis, both HSQC and HMBC experiments were performed on the E–4M1P copolymer richer in 4M1P (36.73 mol%) and are shown in Fig. 4.

The HSQC spectrum, which exhibits correlation between ^1H and ^{13}C atoms having one-bond scalar coupling, was subdivided into three regions, along the proton dimension, for the analysis:

(i) Three cross-peaks are included in the 0.70–0.90 ppm region in Fig. 4a and c. The first cross-peak at $\delta\,^{13}C = 17.87$ ppm ($\delta\,^1H = 0.77$ ppm) is ascribed to the short methyl branch of polyethylene; the second cross-peak at $\delta\,^{13}C = 20.69$ ppm ($\delta\,^1H = 0.80$ ppm) as mentioned before is assigned to the $CH_{3(CW)}$ from 4M1P chain walking; the third signal at $\delta\,^{13}C = 21.18$ ppm ($\delta\,^1H = 0.79$ ppm) is assigned to the $CH_{3}(sc)$ in the E/ 4M1P copolymer. No other signals are detectable in the high field region (from 0.80 to 0.90 ppm) generally assigned to longer methyl or isobutyl branches, thus confirming that the observed resonances in the HSQC experiment can be only ascribed to short methyl branches.

(ii) The proton region spanning from 0.90 to 1.38 ppm shows the methylenes, $T_{\delta\delta}$ and $T_{\beta\delta}$ carbons, already assigned to typical sequences in poly(E-co-4M1P)s.[30–32] Methylene and $\delta\delta$ methine carbon signals assigned to highly branched PE sequences are observed too. Some methylene resonances at $\delta\,^{13}C = 34.38$, 37.27, and 37.74 ppm ($\delta\,^1H = 1.06$, 1.08, and 1.07 ppm) are present (for their assignment see the discussion related to the HMBC experiment).
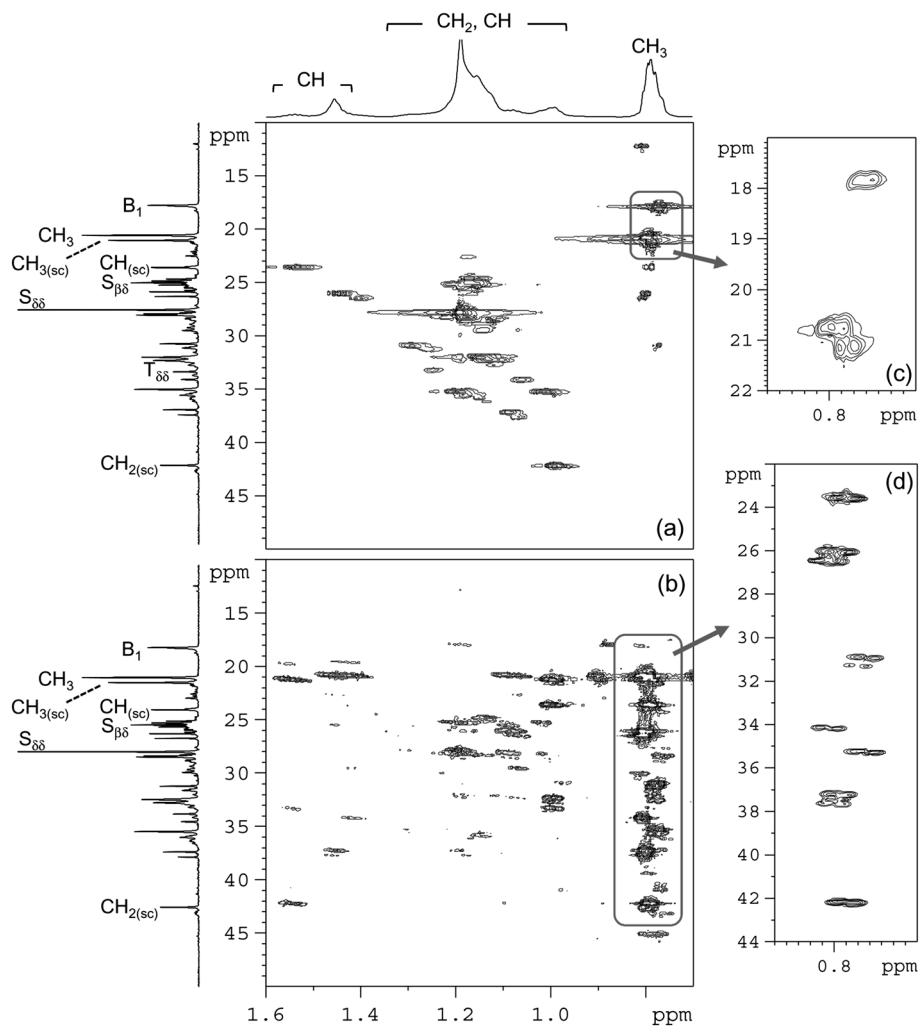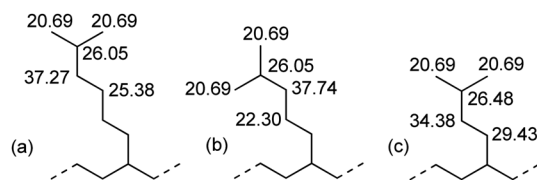

Fig. 4 HSQC (a) and HMBC (b) spectra of an E–4M1P copolymer with 36.73 mol% comonomer content (run 6 in Table 1). The expanded boxes showed the HSQC (c) and HMBC (d) correlations in the methyl proton region. The signal intensity has been reduced 8 times with respect to (a) and (b).

Scheme 6 Possible structures from HMBC analysis and their distinctive chemical shifts: 2-methyl-hexyl (a), 2-methyl-pentyl (b), and 2-methyl-butyl (c).

(iii) The proton region spanning from 1.38 to 1.60 ppm reveals the CH(sc) carbon signal at δ ^{13}C = 23.79 ppm (δ ^{1}H = 1.53 ppm), and two methine signals at δ ^{13}C = 26.05 and 26.48 ppm (δ ^{1}H = 1.44 and 1.40 ppm), respectively assigned in the previous paragraph. The $T_{\beta\beta}$ carbon atom in poly(E-co-4M1P), as well as $T_{\beta\beta}$ of poly(P-co-4M1P), can be once again excluded, because of the lack of the expected ^{1}H and ^{13}C cross-peaks.

Once the direct ^{1}H–^{13}C correlations are assigned, the analysis of the HMBC experiment (Fig. 4b) is of a great help to study the microstructure, assign unknown signals, and determine the comonomer sequences.

HMBC in Fig. 4b reveals the main expected correlations for an E–4M1P copolymer and for PE. Resonances at δ ^{13}C = 26.05, 26.48, 34.38, 37.27, and 37.74 ppm (unknown from the HSQC analysis) can be assigned by observing the methyl proton expanded region of the HMBC spectrum, Fig. 4d. Specifically, the methyl signal at δ ^{13}C = 20.69 ppm (δ ^{1}H = 0.80 ppm) correlates with methine signals at δ ^{13}C = 26.05 and 26.48 ppm respectively, and with the methylene signals at δ ^{13}C = 34.38, 37.27 and 37.74 ppm. These results allow to single out three possible structures: 2-methyl-hexyl (2MH), 2-methyl-pentyl (2MP), and 2-methyl-butyl (2MB), respectively, and to assign, according to Lindeman and Adams, all the corresponding resonances, as reported in Scheme 6.[42]

Homonuclear ^{1}H–^{1}H COSY and ^{1}H–^{1}H TOCSY experiments (see the ESI†) confirm the structures of Scheme 6.

To corroborate the whole set of assignments, the self-consistency check, which is defined as the agreement among the integrals from signals assigned to the same microstructure, was successfully applied.

The complete and detailed ^{13}C NMR assignment is listed in Table 2 and illustrated in Fig. 5, referring to the spectrum of the E/4M1P copolymer with 36.73 mol% comonomer content.

Mechanistic explanation

The copolymerization of E with 4M1P by **Ni-1**/MAO produces a polymer with different types of branching, whose presence can be explained to be a result of: (i) the regiochemistry of the monomer insertion (1,2- or 2,1- insertion of the 4M1P into the Ni-polymer chain growth bond) and (ii) the ability of the metal

Table 2 ^{13}C NMR chemical shift of sequences coming from 4M1P and their assignment

| Carbon	Polymer sequence	Branched units	Branched unit carbon	Chemical shift (ppm)		Ref.
				This work[a]	Literature[b]	
CH$_3$	—	2MH	1	20.69	22.4	14
	—	2MP	1	20.69		This work
	—	2MB	1	20.69		This work
CH$_3$(sc)	EYE/YYE			21.06–21.40		30–32
CH$_3$		2,4MP	10	21.39	23.0–23.2	14
CH$_2$	—	2MP	6	22.30		This work
CH(sc)	EYE/YYE			23.52–23.75		30–32
CH		2,4MP	11	24.42	25.9	14
$S_{\beta\delta}$	YEE			24.81		30–32
CH$_2$	—	2MH	4	25.38	28.2	14
CH	—	2MH	2	26.05	27.8	14
CH	—	2MP	2	26.05		This work
CH	—	2MB	7	26.48		This work
$S_{\delta\delta}$	EEE			27.73		30–32
$S_{\gamma\delta}$	YEEE			28.26		30–32
$S_{\gamma\gamma}$	YEEY			28.81		30–32
CH$_2$	—	2MB	9	29.43		This work
$S_{\alpha\delta}$	YEE			32.54		30–32
$S_{\alpha\gamma}$	YEY			32.84–33.44		30–32
$T_{\delta\delta}$	EYE			33.63		30–32
CH$_2$	—	2MB	8	34.38		This work
CH$_2$	—	2MH	3	37.27	39.4	14
CH$_2$	—	2MP	5	37.74		This work
$S_{\alpha\alpha}$	EYYE			38.87		30–32
CH$_2$(sc)	EYE			42.50		30–32
	YYE			43.02–43.15		30–32
CH$_2$		2,4MP	12	45.24	46.7–48.2	14

[a] At 103 °C; solvent TCE, HMDS internal reference. [b] At 120 °C; solvent o-C$_6$D$_4$Cl$_2$ and o-C$_6$H$_4$Cl$_2$ (volume ratio: 20/80).

center to migrate along the growing polymer chain *via* a series of β-hydride elimination and reinsertion steps.

Specifically, the analysis of the NMR spectra shows that all the branches due to the chain walking mechanism are mostly isolated, due to the absence of signals in the region spanning from 38 to 42 ppm ($S_{\alpha\alpha}$ region). Longer successive 4M1P sequences (triad and over) are not observed even at higher comonomer content, the signals, assigned to $CH_2(sc)$, spanning from 43.12 to 43.67 ppm being absent. Likewise resonances related to the occurrence of a 2,1 insertion after a YY dyad are not detected.

The absence of long comonomer sequences was also pointed out in the homopolymerization of 4M1P with Ni(II) and Pd(II) based catalysts, where this phenomenon was ascribed to the increased rate of chain-walking that was greater with respect to the rate of 4M1P insertion.[14,16] In the poly(E-*co*-4M1P) reaction, the rate of ethylene insertion seems to be generally greater than the rate of chain walking or 4M1P insertion.

Both 1,2 and 2,1 4M1P insertion are allowed with Ni(II) based catalysts, as already observed for 4M1P homopolymerization. However, in E–4M1P copolymerizations, the typical signals related to the 2,1 insertion, such as the $S_{\beta\gamma}$ at 25.31 ppm and $T_{\gamma\delta}$ at 33.97 ppm, corresponding to a YEEY tetrad (**Y** indicates a 2,1 inserted unit), are not detected.[31] This means that (i) 2,1 insertion often leads to chain straightening, *i.e.* after a 2,1 insertion, a chain walking rearrangement is faster than a successive 4M1P or E monomer insertion, (ii) 2,1-insertion, if present, is isolated in the polyethylene chain, thus indistinguishable with respect to a 1,2-insertion, and (iii) adjacent 2,1-insertions without chain-walking are infrequent. Specifically, according to this mechanism, 1,2 insertion results in a 2,5 enchainment, giving two short methyl branches, while the 2,1 insertion results in a 1,5 enchainment with only one methyl branch along the polymer backbone (Scheme 7). Taking into account the results of ^{13}C NMR analysis, a 2,5 polymer chain growth enchainment is not observed. Indeed, the αα methylene at 43.33 ppm (carbon 3 in the 2,5 enchainment of Scheme 7) is not easily detectable. On the other hand, 2-methyl-alkyl
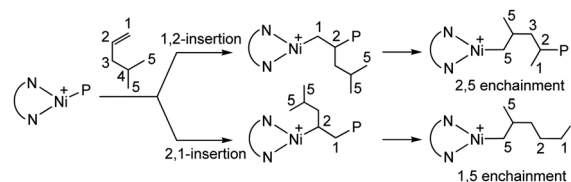
Scheme 7   2,5 and 1,5 enchainment from chain walking.

branches (Scheme 7), coming from the 1,5-enchainment of 4M1P, are observed. These structures are reasonably explained by a subsequent 2,1 insertion and backward migration of the Ni active center along the growing polymer chain. Fewer 2,4-dimethylpentyl branches (<1.0 mol%), coming from 4M1P 1,2 insertion after 1,5-enchainment followed by chain-walking to the growing polymer chain, are observed as suggested by the presence of the αα methylene signal at 45.24 ppm (Scheme 8). Indeed, according to McCord, the nickel active center can migrate backward along the polymer because of the fast chain-walking reaction; hence 2,4-dimethylpentyl branches can be formed.[44]

Conversely, the typical signals coming from 1,5 enchainment of 4M1P are isolated methyl branches along the polymer chain such as B_1, deriving from 2,1 insertion followed by forward migration of the Ni center along the newly inserted monomer. The resonances related to this type of branches are evident in the ^{13}C NMR spectra of the E–4M1P copolymer and in that of PE
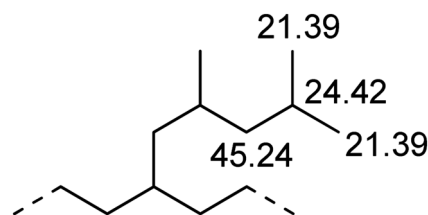
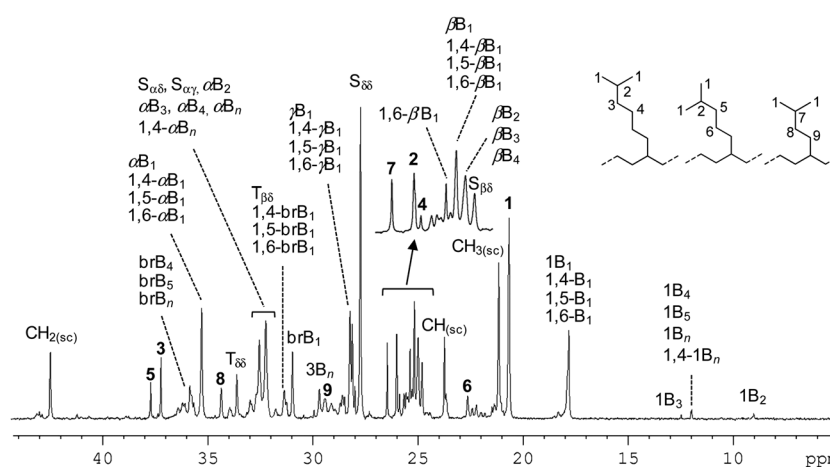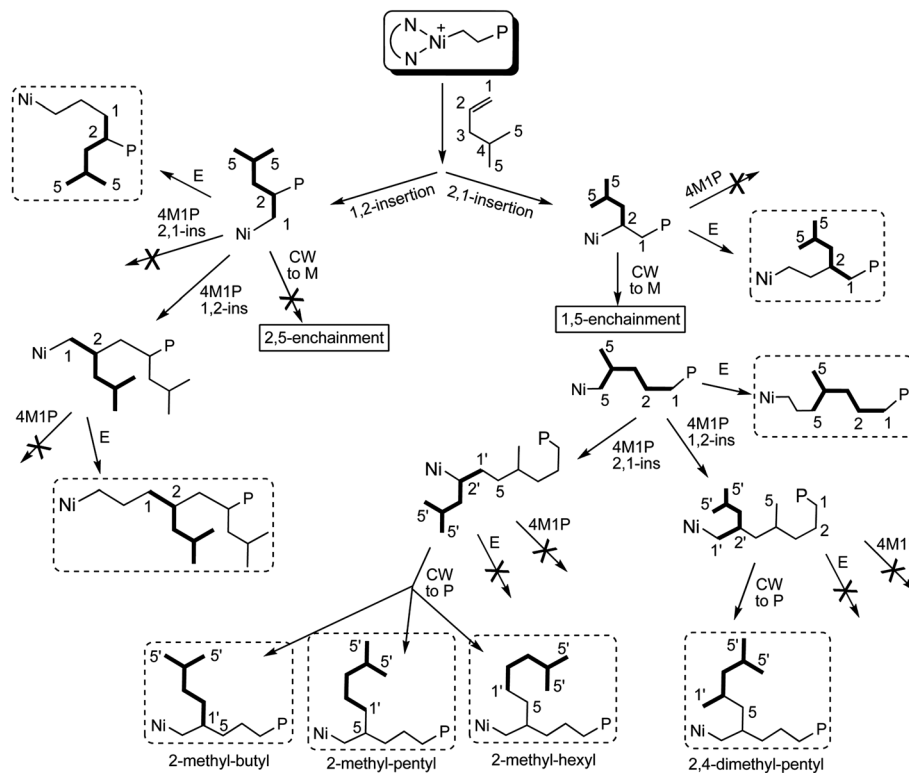Scheme 8   2,4-dimethyl-pentyl branch and its typical resonances.

Fig. 5 ^{13}C NMR spectrum of an E–4M1P copolymer with 36.73 mol% comonomer content (run 6 in Table 1).

Scheme 9 Reaction scheme of an E−4M1P copolymer and observed branches.

too. Thus, it is not possible, at least in principle, to tell apart the signals coming from 4M1P and those from E.

On the whole, the microstructure of E–4M1P copolymers can be reasonably explained by ethylene, 1,2- or 2,1- comonomer insertion and chain-walking mechanism as shown in Scheme 9.

The detailed branched chain distribution is listed in Table 3. For the sake of clarity, the *iso*-butyl group considered as 1,2 inserted 4M1P (sum of 1,2 inserted comonomer and 2,4-dimethylpentyl branches) is quoted among the branches and 4M1P

comonomer content is reported as the sum of all the shares derived from 1,2 and 2,1 inserted units. The amount of each type of branching for E–4M1P copolymers can be obtained from the following relationship:

$$I_i\ (\%) = [I_i/(I_M + I_{Et} + I_P + I_{Bu} + I_{iBU} + I_{2MA} + I_E/2)]100$$

where i is the type of branching under analysis; I_M, I_{Et}, I_P, I_{Bu}, and I_{2MA} are the integrated areas of methyl, ethyl, propyl, butyl,

Table 3 Branched distributions of E−4M1P copolymers obtained by **Ni-1**

| Run/cocatalyst | 4M1P (mol%) | T (°C) | Total branching (%) | Branch distribution | | | | | | | |
				Methyl	Ethyl	Propyl	Butyl	Iso-butyl	2-Methyl-alkyl	Amyl	Long (n ≥ 6)
1/MAO	—	20	47.88	21.89	15.15	2.38	0.08	—	1.26	2.56	4.50
2/MAO	4.87	20	44.28	27.59	3.69	1.87	6.26	1.73	3.14	n.d.	n.d.
3/MAO	10.40	20	56.87	37.42	2.85	1.40	4.80	3.90	6.50	n.d.	n.d.
4/MAO	30.06	20	68.42	32.83	1.42	1.22	2.89	13.76	16.03	n.d.	n.d.
5/MAO	33.52	20	66.16	28.66	1.10	0.85	2.03	14.97	18.55	n.d.	n.d.
6/MAO	36.73	20	71.43	31.01	1.33	0.52	1.83	15.81	20.92	n.d.	n.d.
8/MAO	2.32	0	20.18	14.82	0.65	0.50	1.90	0.81	0.51	n.d.	n.d.
9/MAO	2.13	0	14.12	10.16	0.40	0.37	1.06	0.72	1.41	n.d.	n.d.
10/MAO	3.29	0	27.74	20.23	0.88	0.69	2.64	1.13	2.16	n.d.	n.d.
11/Et₂AlCl	—	20	30.00	17.96	3.02	2.65	0.71	n.d.[a]	0.34	1.83	3.49
12/Et₂AlCl	5.60	0	39.34	27.95	1.02	0.92	3.84	1.69	3.91	n.d.	n.d.
13/Et₂AlCl	15.41	20	63.63	38.87	3.06	1.31	4.98	6.93	8.48	n.d.	n.d.
14/Et₂AlCl	31.65	20	71.05	34.76	1.54	0.89	2.21	14.26	17.39	n.d.	n.d.

[a] n.d. = not detected.

and 2-methyl-alkyl branches; and I_{iBU} and I_E are those related to 4-methyl-1-pentene and ethylene units.

Fig. 6 shows that: (i) the total amount of 2,1 insertion (1,5-enchainment through chain walking and backward migration) is higher than that of 1,2 inserted 4-methyl-1-pentene and (ii) there are no noticeable differences in the amounts of 1,2 and 2,1 inserted units by using MAO or Et$_2$AlCl cocatalyst.

These results are unexpected especially with regard to the amount of 2,1 insertion; indeed in poly(4M1P) by an analogous α-diimine nickel complex, lesser 2,1 insertion occurs with MAO as the cocatalyst, likely due to the different Lewis acidity and bulkiness of the two organoaluminium counteranions.[15,45] Otherwise, a significant increased 2,1 insertion of an α-olefin was already observed for different α-diimine nickel catalysts.[22,24,46]

In addition, Table 3 summarizes the type and the amount of the different branches in E–4M1P copolymers and in poly-(ethylene)s obtained under the same polymerization conditions. As shown in Table 3, poly-(ethylene)s (runs 1 and 11) show a large number of methyl branches besides ethyl, propyl, butyl, amyl and longer branches with six or more carbons. 2-methyl-hexyl branches are present too, as already observed by Galland for polyethylene by an (α-diimine) Nickel catalyst[40] and more evident in polyethylene from MAO (1.26 mol%).

The presence of a comonomer affects not only the total amount of branches in the copolymers but especially the type and the distribution of branches. In the presence of the comonomer we observe: (i) an increase of methyl branches; (ii) a marked decrease of ethyl branches; (iii) the complete absence of branches with five or more carbons; (iv) a sensible increase of 2-methyl-alkyl branches (*i.e.* 2-methyl-butyl, 2-methyl-pentyl, 2-methyl-hexyl, and 2,4-dimethylpentyl branches).

It is worth noting that while fewer 2-methyl-alkyl branches such as isobutyl and 2-methyl-hexyl (not more than 1.1 mol%) were observed in the polyethylene samples produced with (α-diimine) Nickel catalysts as already reported,[39,40] 2-methyl-butyl, 2-methyl-pentyl and 2,4-dimethyl-pentyl branches can be found only in E–4M1P copolymers. The presence of 4M1P as a comonomer and the use of an (α-diimine) Nickel catalyst lead to a branched copolymer quite different from the branched PE homopolymer from the same catalytic system.

Regarding the branching trends of the E–4M1P copolymers, the ^{13}C NMR analysis shows that as the comonomer content

Fig. 7 Methyl branch percentage at different comonomer contents.

increases, the initial amount of methyl, ethyl, propyl and butyl branching increases up to about 20 mol% of 4M1P, which causes a drop in the branching degree. This phenomenon is observed for all the four different types of branching (Fig. 7 and ESI†).

This remark is particularly important with regard to methyl branches, due to the impossibility to distinguish isolated methyl branches deriving from ethylene chain-walking or from typical 1,5 enchainment of 4M1P. In the latter case, an increase in the methyl branching would be expected with increasing comonomer content.

Conclusion

In this work we report on the E–4M1P copolymerization with a **Ni-1** complex in combination with Et$_2$AlCl or MAO. A detailed and complete ^{13}C NMR assignment was conducted, showing a complex copolymer chain architecture. The investigation of the microstructure showed the typical resonances coming from 1,2 insertion together with 2-methyl-alkyl branches coming from 2,1 insertion followed by a fast backward migration of the Ni active center along the growing polymer chain.

The resonance assignment together with the ability to observe newly resolved resonances permitted a more straightforward determination of the structural details in this copolymer and an in-depth understanding of the copolymerization mechanism.

Acknowledgements

Notes and references

1 B. I. Voit and A. Lederer, *Chem. Rev.*, 2009, **109**, 5924–5973.
2 G. J. Domski, J. M. Rose, G. W. Coates, A. D. Bolig and M. Brookhart, *Prog. Polym. Sci.*, 2007, **32**, 30–92.
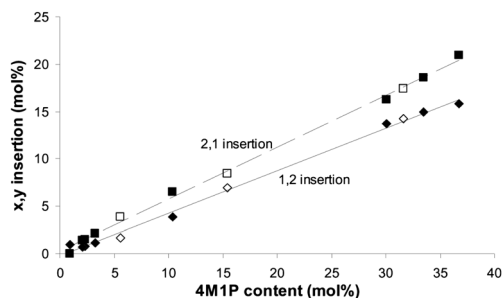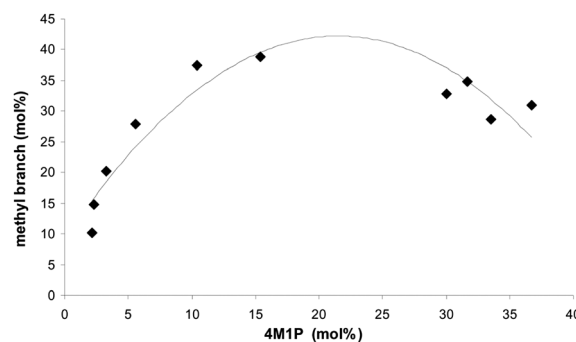3 W. Kaminsky, M. Hoff and S. Derlin, *Macromol. Chem. Phys.*, 2007, **208**, 1341–1348.

Fig. 6 1,2 and 2,1 (1,5-enchainment through chain walking) 4M1P insertion (mol%) with different cocatalysts (empty dots: Et$_2$AlCl, full dots: MAO) at different comonomer contents in the copolymers.

4   G. W. Coates, P. D. Hustad and S. Reinartz, *Angew. Chem., Int. Ed.*, 2002, **41**, 2236–2257.

5   Z. Dong and Z. Ye, *Polym. Chem.*, 2012, **3**, 286–301.

6   G. Sun and Z. Guan, *Macromolecules*, 2010, **43**, 4829–4832.

7   Y. Xu, P. Xiang, Z. Ye and W.-J. Wang, *Macromolecules*, 2010, **43**, 8026–8038.

8   Z. Gao, *Chem. – Eur. J.*, 2002, **8**, 3086–3092.

9   S. D. Ittel, L. K. Johnson and M. Brookhart, *Chem. Rev.*, 2000, **100**, 1169–1203.

10 C. M. Killian, D. J. Tempel, L. K. Johnson and M. Brookhart, *J. Am. Chem. Soc.*, 1996, **118**, 11664–11665.

11 L. K. Johnson, C. M. Killian and M. Brookhart, *J. Am. Chem. Soc.*, 1995, **117**, 6414–6415.

12 Y.-Y. G. Luk, D. A. Foucher and R. A. C. R. Gossage, *Cron. Chim.*, 2013, **16**, 573–579.

13 J. Peleška, Z. Hoštálek, D. Hasalíková and J. Merna, *Polymer*, 2011, **52**, 275–281.

14 H. Gao, J. Pan, L. Guo, D. Xiao and Q. Wu, *Polymer*, 2011, **52**, 130–137.

15 H. Gao, X. Liu, Y. Tang, J. Pan and Q. Wu, *Polym. Chem.*, 2011, **2**, 1398–1403.

16 L. Guo, H. Gao, L. Li and Q. Wu, *Macromol. Chem. Phys.*, 2011, **212**, 2029–2035.

17 S. Zai, F. Liu, H. Gao, C. Li, G. Zhou, S. Cheng, L. Guo, L. Zhang, F. Zhu and Q. Wu, *Chem. Commun.*, 2010, **46**, 4321–4323.

18 J. Merna, Z. Hoštálek, J. Peleška and J. Roda, *Polymer*, 2009, **50**, 5016–5023.

19 J. D. Azoulay, Y. Schneider, G. B. Galland and G. C. Bazan, *Chem. Commun.*, 2009, 6177–6179.

20 D. Meinhard, M. Wegner, G. Kipiani, A. Hearley, P. Reuter, S. Fischer, O. Marti and B. Rieger, *J. Am. Chem. Soc.*, 2006, **129**, 9182–9191.

21 J. M. Rose, A. E. Cherian and G. W. Coates, *J. Am. Chem. Soc.*, 2006, **128**, 4186–4187.

22 A. E. Cherian, J. M. Rose, E. B. Lobkovsky and G. W. Coates, *J. Am. Chem. Soc.*, 2005, **127**, 13770–13771.

23 J.-C. Yuan, L. C. Silva, P. T. Gomes, P. Valerga, J. M. Campos, M. R. Ribeiro, J. C. W. Chien and M. M. Marques, *Polymer*, 2005, **46**, 2122–2132.

24 D. H. Camacho and Z. Guan, *Macromolecules*, 2005, **38**, 2544–2546.

25 J. Merna, J. Cihlar, M. Kucera, A. Deffieux and H. Cramail, *Eur. Polym. J.*, 2005, **41**, 303–312.

26 G. Leone, S. Losio, D. Piovani, A. Sommazzi and G. Ricci, *Polym. Chem.*, 2012, **3**, 1987–1990.

27 A. Bax, R. H. Griffey and B. L. Hawkins, *J. Magn. Reson.*, 1983, **55**, 301–315.

28 A. Bax and S. Subramaniam, *J. Magn. Reson.*, 1986, **67**, 565–569.

29 A. Bax and M. F. Summers, *J. Am. Chem. Soc.*, 1986, **108**, 2093–2094.

30 S. Losio, A. C. Boccia, L. Boggioni, M. C. Sacchi and D. R. Ferro, *Macromolecules*, 2009, **42**, 6964–6971.

31 S. Losio, A. C. Boccia and M. C. Sacchi, *Macromol. Chem. Phys.*, 2008, **209**, 1115–1128.

32 S. Losio, I. Tritto, G. Zannoni and M. C. Sacchi, *Macromolecules*, 2006, **39**, 8920–8927.

33 K. Kakinuki, M. Fujiki and K. Nomura, *Macromolecules*, 2009, **42**, 4585–4595.

34 G. Xu and D. Cheng, *Macromolecules*, 2001, **34**, 2040–2047.

35 G. Leone, A. Boglia, A. C. Boccia, S. Taglialatela Scafati, F. Bertini and G. Ricci, *Macromolecules*, 2009, **42**, 9231–9237.

36 Differences in M_w/M_n could also be due, at least in part, to inaccuracy of M_w and M_n values determined for the branched copolymers. Indeed, both branching and copolymer composition affect the hydrodynamic volume of a polymer in a particular solvent. Because SEC separates by hydrodynamic volume, not by molecular weight, this results in co-elution of chains of different molecular weights (but same hydrodynamic volume) at a given elution time. See for example M. Gaborieau and P. Castignolles, *Anal. Bioanal. Chem.*, 2011, **399**, 1413–1423.

37 T. Usami and S. Takayama, *Macromolecules*, 1984, **17**, 1756–1761.

38 C. J. Carman and C. E. Wilkes, *Rubber Chem. Technol.*, 1971, **44**, 781–804.

39 G. B. Galland, R. F. de Souza, R. Santos Mauler and F. F. Nunes, *Macromolecules*, 1999, **32**, 1620–1625.

40 L. C. J. Ferreira, P. A. Melo, G. L. Crossetti, G. B. Galland, M. Nele and J. C. Pinto, *Polym. Eng. Sci.*, 2010, **50**, 1797–1808.

41 To date, a deeper comparison between 4M1P homopolymerization from Pd and Ni based catalysts is not possible due to the restricted presence of experimental data and the heterogeneity of such data coming from polymerizations conducted under different conditions *i.e.* temperature, cocatalyst, cocatalyst/catalytic system ratio, solvent.

42 L. P. Lindeman and J. Q. Adams, *Anal. Chem.*, 1971, **43**, 1245–1251.

43 S. Losio, A. C. Boccia, F. Forlini and M. C. Sacchi, *Macromolecules*, 2011, **44**, 3276–3286.

44 E. F. Mc Cord, S. J. McLain, L. T. J. Nelson, S. D. Arthur, E. B. Coughlin, S. D. Ittel, L. K. Johnson, D. Tempel, C. M. Killian and M. Brookhart, *Macromolecules*, 2001, **34**, 362–371.

45 R. F. de Souza, L. C. Simon, M. do Carmo and M. Alves, *J. Catal.*, 2003, **214**, 165–168.

46 F. Liu, H. Gao, Z. Hu, H. Hu, F. Zhu and Q. Wu, *J. Polym. Sci., Part A: Polym. Chem.*, 2012, **50**, 3859–3866.